Am J Physiol Heart Circ Physiol 290: H2516–H2521, 2006.
First published January 13, 2006; doi:10.1152/ajpheart.01038.2005.

Multimodal functional cardiac MRI in creatine kinase-deficient mice reveals subtle abnormalities in myocardial perfusion and mechanics

Matthias Nahrendorf,[1,2] Jörg U. Streif,[2] Karl-Heinz Hiller,[2] Kai Hu,[1] Peter Nordbeck,[1] Oliver Ritter,[1] David Sosnovik,[3] Lisa Bauer,[1] Stefan Neubauer,[4] Peter M. Jakob,[2] Georg Ertl,[1] Matthias Spindler,[1] and Wolfgang R. Bauer[1]

[1]*Medizinische Klinik und Poliklinik 1 and* [2]*Physikalisches Institut, Universität Würzburg, Würzburg, Germany;* [3]*Martinos Center for Biomedical Imaging, Massachusetts General Hospital, Harvard Medical School, Charlestown, Massachusetts; and* [4]*Department of Cardiovascular Medicine, John Radcliffe Hospital, Oxford University, Oxford, United Kingdom*

Submitted 3 October 2005; accepted in final form 12 January 2006

Nahrendorf, Matthias, Jörg U. Streif, Karl-Heinz Hiller, Kai Hu, Peter Nordbeck, Oliver Ritter, David Sosnovik, Lisa Bauer, Stefan Neubauer, Peter M. Jakob, Georg Ertl, Matthias Spindler, and Wolfgang R. Bauer. Multimodal functional cardiac MRI in creatine kinase-deficient mice reveals subtle abnormalities in myocardial perfusion and mechanics. *Am J Physiol Heart Circ Physiol* 290: H2516–H2521, 2006. First published January 13, 2006; doi:10.1152/ajpheart.01038.2005.—A decrease in the supply of ATP from the creatine kinase (CK) system is thought to contribute to the evolution of heart failure. However, previous studies on mice with a combined knockout of the mitochondrial and cytosolic CK ($CK^{-/-}$) have not revealed overt left ventricular dysfunction. The aim of this study was to employ novel MRI techniques to measure maximal myocardial velocity (V_{max}) and myocardial perfusion and thus determine whether abnormalities in the myocardial phenotype existed in $CK^{-/-}$ mice, both at baseline and 4 wk after myocardial infarction (MI). As a result, myocardial hypertrophy was seen in all $CK^{-/-}$ mice, but ejection fraction (EF) remained normal. V_{max}, however, was significantly reduced in the $CK^{-/-}$ mice [wild-type, 2.32 ± 0.09 vs. $CK^{-/-}$, 1.43 ± 0.16 cm/s, $P < 0.05$; and wild-type MI, 1.53 ± 0.11 vs. $CK^{-/-}$ MI, 1.26 ± 0.11 cm/s, P = not significant (NS), $P < 0.05$ vs. baseline]. Myocardial perfusion was also lower in the $CK^{-/-}$ mice (wild-type, 6.68 ± 0.27 vs. $CK^{-/-}$, 4.12 ± 0.63 ml/g·min, $P < 0.05$; and wild-type MI, 3.97 ± 0.65 vs. $CK^{-/-}$ MI, 3.71 ± 0.57 ml/g·min, P = NS, $P < 0.05$ vs. baseline), paralleled by a significantly reduced capillary density (histology). In conclusion, myocardial function in transgenic mice may appear normal when only gross indexes of performance such as EF are assessed. However, the use of a combination of novel MRI techniques to measure myocardial perfusion and mechanics allowed the abnormalities in the $CK^{-/-}$ phenotype to be detected. The myocardium in CK-deficient mice is characterized by reduced perfusion and reduced maximal contraction velocity, suggesting that the myocardial hypertrophy seen in these mice cannot fully compensate for the absence of the CK system.

magnetic resonance imaging; contractility; myocardial infarction

CHANGES IN myocardial energetics, including reduced levels of phosphocreatine, creatine kinase (CK) (10, 16), and ATP (20), have been documented in the failing heart. However, whether these alterations in myocardial energetics are a causal mechanism contributing to left ventricular (LV) remodeling and dysfunction or an adaptive phenomenon has yet to be resolved. Recently, our group reported that deletion of the CK enzyme system [double knockout of the mitochondrial and cytosolic CK ($CK^{-/-}$)] leads to adaptive changes of the murine heart, consisting of LV hypertrophy and mild dilatation of the LV. However, cardiac output and LV ejection fraction remained normal in these mice (15). Furthermore, when $CK^{-/-}$ mice were examined 4 wk after the induction of myocardial infarction (MI), no evidence of adverse LV remodeling was seen (15). Therefore, the aim of the current study was to determine whether the use of novel techniques in mouse cardiac MRI, such as perfusion imaging and the imaging of myocardial mechanics, would allow subtle abnormalities of the myocardial phenotype to be detected.

A phase-contrast MRI pulse sequence, recently developed by our group (21) to measure myocardial contraction velocity and mechanics in mice, was used in this study. In addition, a second novel MR technique to quantify myocardial perfusion, which has also recently been modified to work in the small and rapidly beating mouse heart (12, 22), was employed to assess myocardial perfusion in the $CK^{-/-}$ mice. A reduction in myocardial perfusion in hypertrophied hearts may be a significant risk for the development of systolic dysfunction over time (13, 25), and the quantification of myocardial perfusion is thus important in the assessment of transgenic mice with LV hypertrophy, such as the $CK^{-/-}$ mice.

The hypothesis tested in this study was that LV hypertrophy, induced by deletion of CK isozymes, might be associated with impaired myocardial perfusion and impaired myocardial contraction velocity. In addition, MI was induced in both wild-type (WT) and CK-deficient mice to compare the changes caused by CK deficiency to those of post-MI ventricular remodeling.

METHODS

Animals and experimental protocol. CK-deficient mice were obtained from Dr. Bé Wieringa (University of Nijmegen, The Netherlands). A total of 14 female and 15 male mice of a mean age of 41 ± 2 wk were studied. CK-deficient mice had a mixed C57Bl/6–129/Sv background, and WT mice were C57Bl/6. The investigation conformed to the *Guide for the Care and Use of Laboratory Animals*, published by the National Institutes of Health (NIH Publications No. 85-23, Revised 1996) and was approved by the insitutional local ethics committee. A complete in vivo MRI study (see below) was performed in six WT and seven $CK^{-/-}$ mice. In addition, eight WT and eight $CK^{-/-}$ mice that were subjected to left coronary artery ligation as described previously (7) were studied 4 wk after MI.

Address for reprint requests and other correspondence: W. R. Bauer, Medizinische Klinik und Poliklinik 1, Universität Würzburg, Josef Schneider-Str. 2, 97080 Würzburg, Germany (e-mail: bauer_w@medizin.uni-wuerzburg.de).

The costs of publication of this article were defrayed in part by the payment of page charges. The article must therefore be hereby marked "*advertisement*" in accordance with 18 U.S.C. Section 1734 solely to indicate this fact.

Cine MRI. All experiments were performed on a Bruker Biospec 70/20 scanner at 7.05 T under inhalation anesthesia applied by a nose cone [1.5% isoflurane, supplemented with oxygen (0.5 l/min)]. Depending on the individual heart rate, the entire duration of the acquisition of all MRI data was ~50 min per animal (spin-labeling MRI, 30 min; velocity-encoded cine MRI, 10 min; and multislice cine MRI, 10 min). Cine and phase contrast MRIs were performed by using a custom-made circularly polarized radiofrequency resonator in birdcage design with an inner diameter of 35 mm. An ECG-triggered fast gradient echo cine sequence was used with the following imaging parameters: echo time, 1.5 ms; repetition time, 4.3 ms; field of view, 30 mm^2; acquisition matrix, 128 × 128; and slice thickness, 1.0 mm (17). Contiguous ventricular short-axis slices (n = 10–12; 1 mm thick) were acquired to cover the entire heart. Myocardial infarct size was determined for every slice as the area of myocardium with significant thinning, akinesia, or dyskinesia (15). The ejection time was estimated by counting the frames between the end-diastolic and end-systolic image in the midventricular short-axis slice. This number was then multiplied with the interframe time of the individual scan.

Spin-labeling perfusion MRI. The principles underlying arterial spin labeling have been described extensively elsewhere (3). This technique has been validated against microspheres (9, 25) and first pass perfusion imaging with gadolinium in rats (2) and has recently been performed in mice. In brief, the technique consists of the acquisition of two successive inversion recovery images. The first image employs a nonselective inversion prepulse, whereas the second prepulse is slice selective. Postprocessing of these two images allows a perfusion map to be calculated.

We used a dedicated coil combination consisting of a mouse body coil in birdcage design for transmission and a surface coil for detection of the signal. The relaxation time T1 (T1) quantification was performed using a segmented ECG-gated inversion recovery snapshot fast low-angle shot (FLASH) sequence with a echo time (TE) of 1.5 ms and a repetition time of 2.6 ms. Because minimal heart motion as well as maximum myocardial perfusion occurs during diastole, the image acquisition was performed during this period of the cardiac cycle. After the initial spin inversion with an adiabatic hyperbolic secant inversion pulse, 48 k-space segments were acquired to track the relaxation of the magnetization. A flip angle between 3° and 5° was chosen for this series of FLASH images. The field of view was 30 × 30 mm, the imaging slice thickness was 2 mm, and the radiofrequency excitation was performed with a sinc-shaped pulse with a duration of 500 μs. For slice selective inversion, the inversion slice thickness was adjusted to 6 mm. The detection slice for the T1 measurement was positioned in a midventricular short-axis view. To increase the signal-to-noise ratio (SNR), 16 signal averages were performed. All postprocessing was performed as described before (22) using Interactive Data Language (Research Systems, Boulder, CO). Interpolation was used to derive perfusion maps with a nominal resolution of 234 × 234 μm, and perfusion values were calculated in a transmural region of interest. Because the subendocardial layer of pixels is prone to partial volume effects from the blood pool, care was taken not to include this layer in the region of interest. In mice that were studied postinfarction, the perfusion was measured in a region of interest comprising only the remote myocardium with the infarct zone excluded.

Phase-contrast MRI for contraction velocity measurement. Murine phase-contrast MRI was performed by using a segmented FLASH imaging sequence, as described in detail previously (21). A comparable approach using displacement encoding with stimulated echoes has been proposed for use in mice by Gilson et al. (8). To reduce motion artifacts, this sequence was velocity compensated in all three dimensions by using rephasing gradients (21). Velocity encoding factor was produced by using bipolar gradient pulses, which resulted in a linear dependence between the voxel velocity and spin phase. Imaging parameters were as follows: velocity encoding factor, 6 cm/s; field of view, 30 × 30 mm; matrix size, 128 × 128 (image resolution of 234 × 234 μm); slice thickness, 1 mm; TE, 3.0 ms; and number of signal averages, 4. The acquisition was ECG-gated, and 20 image frames in a midventricular short-axis view were obtained over at least 110% of the R-R interval to cover a full heart cycle. The total acquisition time for the five datasets was ~10 min, depending on the individual heart rate. Two different kinds of maps were calculated from the phase contrast data: magnitude maps, which were used for quantification of myocardial velocity, and vector maps for the visualization of the myocardial mechanics (21).

Histological assessment of capillary density. To determine whether changes in myocardial perfusion were caused by structural or functional changes in the myocardium of the CK-deficient mice, we determined the capillary density histologically by staining endothelial cells with BS-I Isolectin B4. Sections (4 μm thick) were deparaffinized and rehydrated, and endogenous peroxidase was inhibited by H_2O_2 (0.3%) for 15 min. The sections were incubated overnight with the biotinylated lectin. In a second step, the signal was then intensified with an avidin-biotin-complex containing peroxidase-labeled biotins (Lab Vision, Fremont, CA). Finally, the sections were incubated with diaminobenzidine solution. Endothelial cells of capillaries and larger vessels were visualized in the myocardium as a brown precipitate. Capillary density in the viable LV wall was calculated as the number of capillaries per tissue area.

Statistics. Analysis of data was performed in a blinded fashion. Data are expressed as means ± SE. Statistical comparisons among various groups were evaluated by ANOVA, followed by Duncan's test to isolate significance of differences between individual means. $P < 0.05$ was considered to indicate statistical significance.

RESULTS

Cine MRI. Representative examples of a diastolic short-axis view of a WT and $CK^{-/-}$ mouse heart are shown in Fig. 1. We found a marked increase in LV mass in $CK^{-/-}$ compared with WT mice (159.4 ± 8.6 vs. 99.6 ± 4.2 mg, $P < 0.05$), but

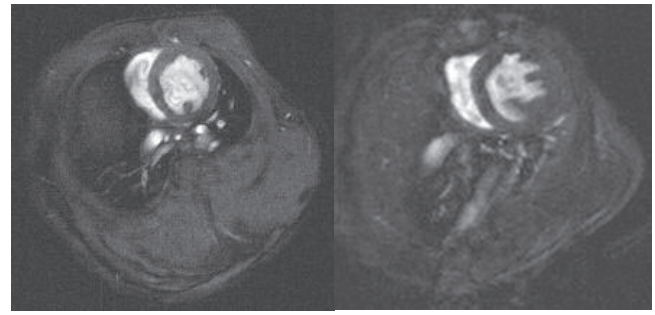

Diastolic short axis view of a wild type (left) and $CK^{-/-}$ mouse heart

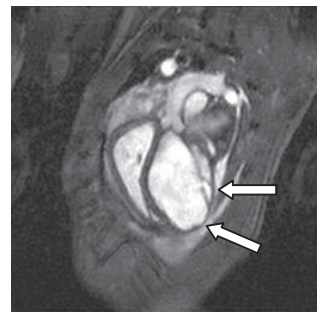

Diastolic long axis view of a wild type heart with MI (arrow).

Fig. 1. Typical diastolic short-axis view of a wild-type (*top*, *left*) and double knockout of the mitochondrial and cytosolic creatine kinase ($CK^{-/-}$; *top*, *right*) mouse heart, which were used to determine left ventricular (LV) mass and volumes. LV hypertrophy is clearly visible in the CK-deficient mouse. *Bottom*: diastolic long-axis view of a wild-type heart after myocardial infarction (MI; arrow).

ejection fraction was normal in the $CK^{-/-}$ mice [WT, 62 ± 3%; and $CK^{-/-}$, 62 ± 4%, P = not significant (NS)], consistent with our prior observations (15). Infarct size in the WT and $CK^{-/-}$ mice was similar (31 ± 7 vs. 30 ± 2%) after exclusion of two of the WT mice with the largest infarcts. The reduction in ejection fraction post-MI was not greater in the $CK^{-/-}$ mice compared with WT mice (WT MI, 39 ± 6%; and $CK^{-/-}$, 37 ± 4%, $P < 0.05$ vs. control). In addition, LV mass was similar in WT and $CK^{-/-}$ mice (WT MI, 171.5 ± 13.9 mg; and $CK^{-/-}$ MI, 160.7 ± 10.5 mg, $P < 0.05$ vs. WT control) 4 wk after MI. No significant differences in cardiac output, body weights, and heart rates (452 ± 18 for all mice during MRI) were detected between the groups (data not shown).

The ejection time was increased in $CK^{-/-}$ mice and in mice with MI (WT, 55 ± 5 ms; WT MI, 67 ± 5 ms; $CK^{-/-}$, 74 ± 6 ms; and $CK^{-/-}$ MI, 79 ± 10 ms, $P < 0.05$ for WT vs. $CK^{-/-}$ and $CK^{-/-}$ MI).

Spin-labeling perfusion MRI. As depicted in Fig. 2, myocardial perfusion was significantly diminished in CK-deficient mice at baseline, as well as in the remote areas of myocardium in all mice after the induction of MI. Perfusion was reduced to the same extent after infarction in both the WT and $CK^{-/-}$ mice. Perfusion values in the myocardium were also found to be inversely correlated to increase in LV mass in all mice (Fig. 4*A*).

Phase-contrast MRI. Maximal myocardial contraction velocity was significantly reduced in the $CK^{-/-}$ versus WT mice, despite similar ejection fractions in the two groups. A similar decrease in contraction velocity was noted in the $CK^{-/-}$ hearts at baseline and in the remodeled areas of WT myocardium, remote from the infarct (Fig. 3). Diastolic myocardial velocity was diminished in parallel to systolic velocity (Fig. 3). Maximum contraction velocity was inversely correlated to the increase in LV mass (Fig. 4*B*), as was seen with myocardial perfusion. The velocity vector map also revealed a loss of the normal twisting motion during systole in both the $CK^{-/-}$ and the post-MI mice.

Effect of $CK^{-/-}$ and MI on cardiac capillary density. $CK^{-/-}$ hearts had significantly fewer capillaries (1,187 ± 61 cap/mm^2) compared with WT controls (2,224 ± 51 cap/mm^2; $P < 0.05$), as shown in Fig. 5. Post-MI remodeling also reduced capillary density in the remote myocardium of WT mice significantly (1,342 ± 98 cap/mm^2; $P < 0.05$) compared with

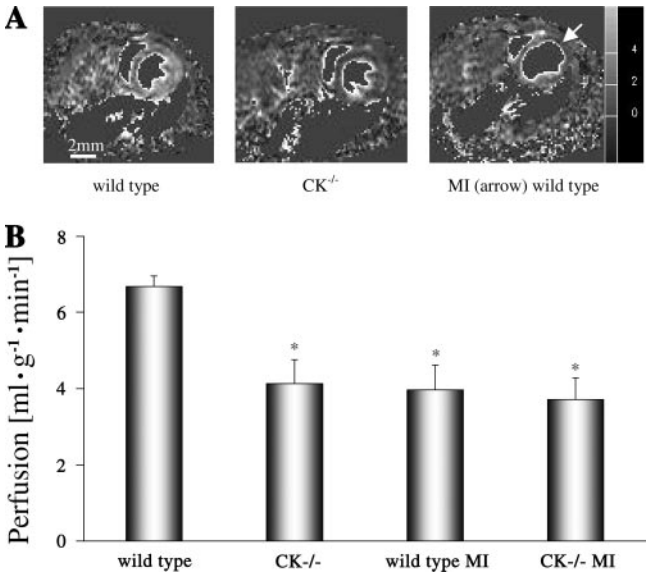

Fig. 2. *A*: perfusion maps (ml·g^{-1}·min^{-1}) of a wild-type mouse (*left*), a $CK^{-/-}$ mouse (*middle*), and a wild-type mouse 4 wk after MI (*right*, arrow). In CK-deficient mouse, as well as in remote myocardium of the wild-type mouse after MI, perfusion values are lower than those in the wild-type mouse. In the anterolateral infarct scar, perfusion values are even further diminished. Layer of pixels bordering LV cavity appears bright, which is most likely due to partial volume effects caused by high rate of spin refreshment in LV cavity. These pixels were not included in the analysis. *B*: absolute perfusion values (ml·g^{-1}·min^{-1}) are significantly diminished in CK-deficient mice and in remote zone of mice after MI. Data represent means ± SE. *$P < 0.05$ vs. wild-type control.

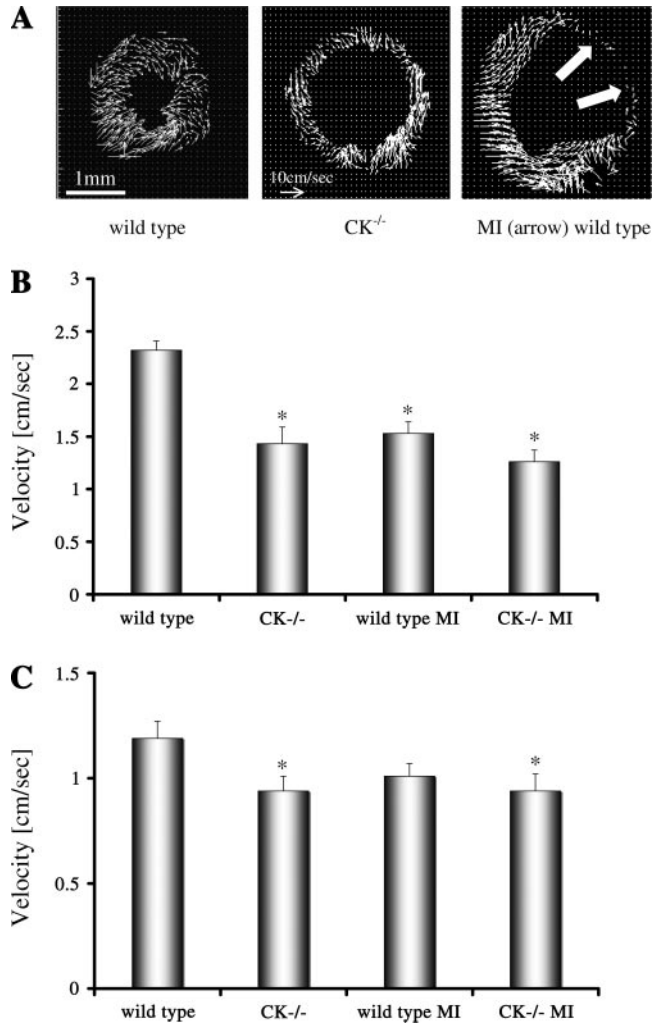

Fig. 3. *A*: vector maps, acquired by phase-contrast MRI, displaying both direction (arrowhead) and amplitude (length of arrow) of myocardial motion. Systolic short-axis image in wild-type control (*left*) mouse displays wringing motion characteristic of normal systolic contraction. Magnitude of myocardial contraction velocity is significantly reduced in the CK-deficient mouse (*middle*), and normal wringing motion in systole is attenuated. Contraction velocity is dramatically reduced in infarct zone of wild-type mouse (*right*) but also reduced in remote myocardium. Myocardial wringing is also attenuated in mice with MI. *B*: maximum contraction velocity of remote region (in cm/s) is significantly diminished in CK-deficient mice and mice after MI. Data represent means ± SE. *$P < 0.05$ vs. wild-type control. *C*: maximum diastolic relaxation velocity of remote region (in cm/s) is diminished in CK-deficient mice and mice after MI. Data are means ± SE. *$P < 0.05$ vs. wild-type control.

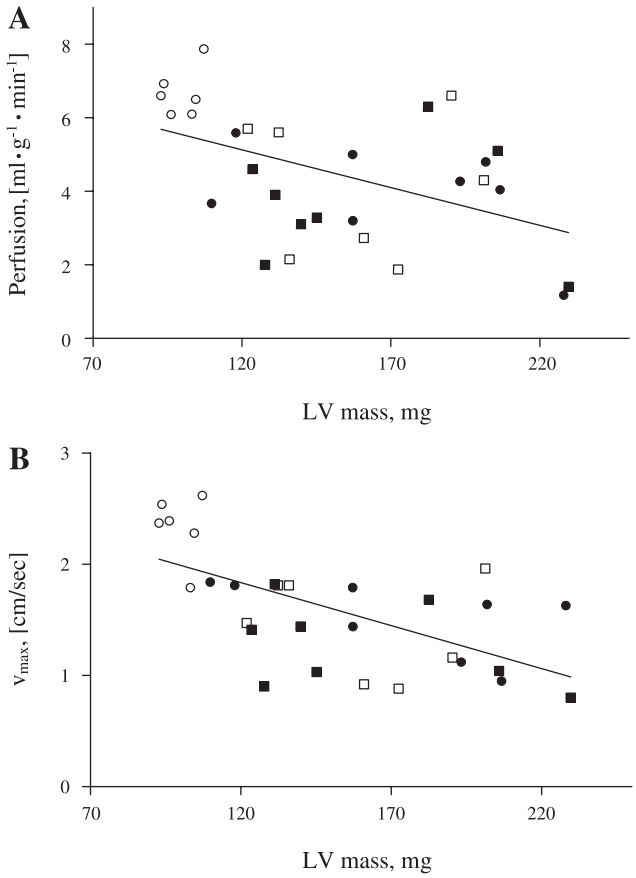

Fig. 4. *A*: perfusion values of remote region were found to be inversely correlated to LV mass: Perfusion = $-0.02 \cdot LV_{mass} + 7.6$; $R^2 = 0.23$; and $P < 0.01$. Wild-type control (○), wild-type MI (●), $CK^{-/-}$ control (□), and $CK^{-/-}$ MI (■) are shown. *B*: maximum contraction velocity was inversely correlated to LV mass: maximal myocardial velocity $V_{max} = -0.008 \cdot LV_{mass} + 2.8$; $R^2 = 0.39$; and $P < 0.01$.

WT control. However, $CK^{-/-}$ mice subject to MI did not display a reduction in capillary density in the remote myocardium compared with control knockout mice ($CK^{-/-}$ with MI, 1,222 ± 116 cap/mm^2; P = NS vs. $CK^{-/-}$ control).

DISCUSSION

The generation of transgenic mice plays a critical role in investigating the mechanisms of myocardial disease, and ventricular function in these mice is often assessed in vivo by measuring ejection fraction or fractional shortening by echo. However, as shown in this study, these traditional indexes of ventricular function may not be able to detect mild myocardial dysfunction, especially under basal conditions. The use of a combination of novel functional cardiac MRI modalities in this study allowed significant abnormalities in myocardial function to be detected in the $CK^{-/-}$ model. Spin-labeling perfusion MRI showed reduced myocardial perfusion in these CK-deficient mice, and maximal systolic myocardial contraction velocity was also significantly diminished, although ejection fraction was preserved.

Myocardial perfusion in our study was inversely correlated to LV mass in the $CK^{-/-}$ hearts and the post-MI remodeled hearts. The most likely reason for this phenomenon is a reduced relative capillary density in the hypertrophied hearts

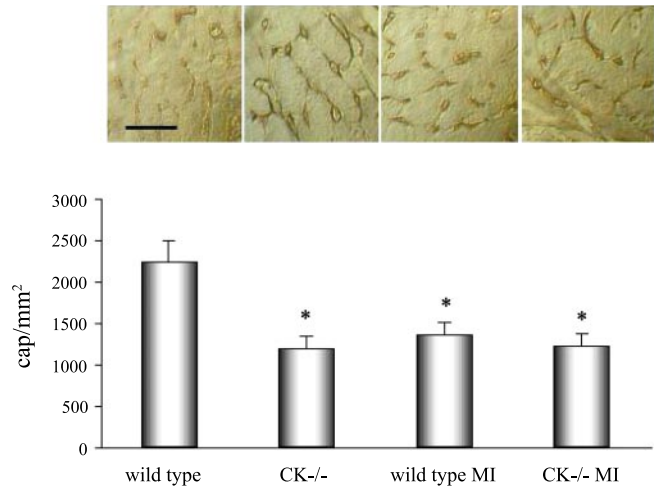

Fig. 5. Lectin-stained sections from noninfarcted segments of LV wall obtained from different experimental groups showing individual capillaries. *Top*: original histology photographs. *Bottom*: number of counted capillaries/mm^2 (cap/mm^2). Bar (in *top*, *left*) indicates 10 μm for all photographs. Magnification is ×500. Capillary density was found to be reduced significantly in CK-deficient mice and in remote zones of wild-type mice after MI. *$P < 0.05$.

(Fig. 5). An increase in myocyte cross-sectional area of 30% has previously been reported in $CK^{-/-}$ mice (15). Ultrastructurally, this was accompanied by abundant and disorganized mitochondria located next to the myofibrils (11). Thus, whereas the myocytes in these hearts undergo hypertrophy, the number of capillaries does not increase, and a demand/supply mismatch may ensue. In rats, a reduction in capillary density has also been described in the hypertrophied areas of remodeled myocardium (1) and has been demonstrated to result in diminished perfusion values (24). This reduction in perfusion may place the myocardium remote from the infarct under even further stress and contribute to the evolution of heart failure.

Whereas global LV function was unaffected by CK deficiency, maximum contraction velocity was significantly slower and correlated inversely with LV mass (Fig. 4*B*) and with myocardial perfusion ($r = 0.34$, $P = 0.02$). This phenomenon

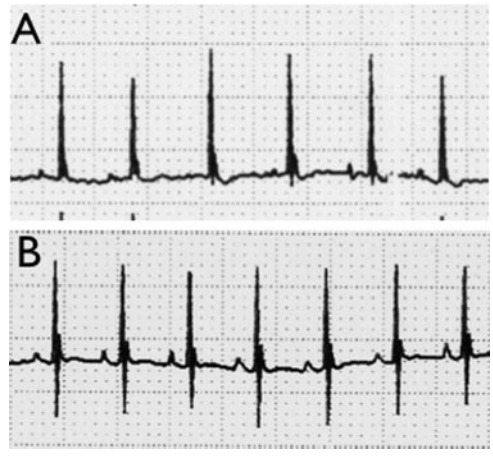

Fig. 6. *A*: ECG of wild-type mouse. Time scale is 50 mm/s. *B*: as shown in the depicted example ECG of a $CK^{-/-}$ mouse, the QRS complex was found to be narrow, making conduction disorders such as bundle brunch block unlikely to cause slower contraction velocity. No apparent differences with wild-type mice were found.

was also seen in WT and CK-deficient mice with MI, but in these animals global LV function was affected as well. In line with the phase-contrast data, the systolic ejection time was prolonged in all mice with decreased peak contraction velocities. The presence of reduced myocardial contraction velocities in patients with cardiac hypertrophy has been shown to predict the development of subsequent heart failure (25). Likewise, a reduction in V_{max} might be an early sign preceding global failure of the LV in some mouse models of myocardial hypertrophy. However, it should be noted that at the present time it is not known whether CK-deficient mice develop heart failure as they age. Therefore, the possibility of stable LV hypertrophy in this model, despite reduced myocardial velocities, cannot be excluded.

The diminished maximum contraction velocity in the $CK^{-/-}$ mice can be correlated with the analysis of the myosin heavy chain (MHC) isoforms in our previous work. A significant reexpression of β-MHC, as a marker of cardiac hypertrophy (18), was detected in CK-deficient mice and in mice with chronic MI (15). The isoform switch is associated with alterations in the functional and energetic behavior of the contractile apparatus: whereas α-MHC leads to a higher maximal shortening velocity but to lower energy economy, high amounts of β-MHC decrease maximal shortening velocity, which indeed was demonstrated by phase-contrast MRI in our study.

Lower myocardial velocities may also be caused by conduction abnormalities such as a bundle brunch block. However, we did not find baseline ECG abnormalities in CK-deficient mice (example ECG, Fig. 6) or observe overt bundle branch block during the MRI scans, which makes this mechanism unlikely.

The development of abnormal myocardial function in areas of myocardium remote from the infarct zone is a well-documented feature of the remodeling process. The mice subjected to MI in our study developed eccentric LV hypertrophy as expected and described previously (28); however, myocardial perfusion and capillary density were significantly reduced in these hypertrophied zones. This imbalance between myocardial demand and perfusion may result in cardiomyocyte apoptosis and a progressive loss of function in these zones. Therapies to improve vascular supply and myocardial perfusion in remote zones of remodeling myocardium may thus provide a strategy to attenuate the remodeling process.

$CK^{-/-}$ mice were previously reported to have increased susceptibility to ischemic injury in the setting of the isolated perfused heart model (19). On the other hand, LV dilatation after MI is not aggravated in $CK^{-/-}$ mice (15), and we found a similar decline in myocardial perfusion (Fig. 2) and myocardial velocities (Fig. 3). These conflicting findings at first sight may be explained by the design of our chronic studies: animals were matched for infarct size at a late time point (4 wk) to control for this powerful confounder of remodeling. Therefore, no conclusions can be drawn about acute infarct healing, which is probably best assessed by a comparison of the acute area at risk to the resulting chronic infarct size.

The use of advanced MRI techniques to characterize seemingly normal myocardium is well described in large mammals and humans. Despite the presence of a normal ejection fraction in patients with obesity (6), significant abnormalities were detected in myocardial mechanics by MRI. In addition, measurement of myocardial velocities by tissue Doppler imaging (14, 23) has been described to detect early changes in large animal heart failure models (5) and patients (27) and has been shown to possess predictive value (26). Blood oxygen level dependent MRI has demonstrated a significant decrease in myocardial flow reserve in hypertrophied hearts (4) despite normal resting function. The data and techniques described in this study of a transgenic mouse are thus directly translatable and relevant to human pathology and a broad array of common cardiac diseases.

In conclusion, the use of a comprehensive MRI technique, including perfusion and motion velocity measurements, allowed abnormalities in myocardial function to be detected in CK knockout mice. Importantly, traditional indexes of myocardial function, such as ejection fraction, did not have the ability to detect the abnormalities in myocardial function in these mice. Phenotypic characterization of transgenic mice should thus include measurements of myocardial perfusion and motion velocity in addition to traditional parameters, such as ejection fraction.

ACKNOWLEDGMENTS

We gratefully acknowledge Prof. B. Wieringa, who provided various breeding pairs of CK-deficient mice.

GRANTS

This work was supported by Deutsche Forschungsgemeinschaft, Sonderforschungsbereich "Pathophysiologie der Herzinsuffizienz" SFB-355 and by the British Heart Foundation.

REFERENCES

1. **Anversa P, Olivetti G, and Capasso JM.** Cellular basis of ventricular remodeling after myocardial infarction. *Am J Cardiol* 68: 7D–16D, 1991.
2. **Bauer WR, Hiller KH, Galuppo P, Neubauer S, Kopke J, Haase A, Waller C, and Ertl G.** Fast high-resolution magnetic resonance imaging demonstrates fractality of myocardial perfusion in microscopic dimensions. *Circ Res* 88: 340–346, 2001.
3. **Bauer WR, Hiller KH, Roder F, Rommel E, Ertl G, and Haase A.** Magnetization exchange in capillaries by microcirculation affects diffusion-controlled spin-relaxation: a model which describes the effect of perfusion on relaxation enhancement by intravascular contrast agents. *Magn Reson Med* 35: 43–55, 1996.
4. **Beache GM, Herzka DA, Boxerman JL, Post WS, Gupta SN, Faranesh AZ, Solaiyappan M, Bottomley PA, Weiss JL, Shapiro EP, and Hill MN.** Attenuated myocardial vasodilator response in patients with hypertensive hypertrophy revealed by oxygenation-dependent magnetic resonance imaging. *Circulation* 104: 1214–1217, 2001.
5. **Chetboul V, Escriou C, Tessier D, Richard V, Pouchelon JL, Thibault H, Lallemand F, Thuillez C, Blot S, and Derumeaux G.** Tissue Doppler imaging detects early asymptomatic myocardial abnormalities in a dog model of Duchenne's cardiomyopathy. *Eur Heart J* 25: 1934–1939, 2004.
6. **Danias PG, Tritos NA, Stuber M, Kissinger KV, Salton CJ, and Manning WJ.** Cardiac structure and function in the obese: a cardiovascular magnetic resonance imaging study. *J Cardiovasc Magn Reson* 5: 431–438, 2003.
7. **Frantz S, Hu K, Widder J, Bayer B, Witzel CC, Schmidt I, Galuppo P, Strotmann J, Ertl G, and Bauersachs J.** Peroxisome proliferator activated-receptor agonism and left ventricular remodeling in mice with chronic myocardial infarction. *Br J Pharmacol* 141: 9–14, 2004.
8. **Gilson WD, Yang Z, French BA, and Epstein FH.** Complementary displacement-encoded MRI for contrast-enhanced infarct detection and quantification of myocardial function in mice. *Magn Reson Med* 51: 744–752, 2004.
9. **Hiller KH, Roder F, Adami P, Voll S, Kowallik P, Haase A, Ertl G, and Bauer WR.** Study of microcirculation by coloured microspheres and NMR-microscopy in isolated rat heart: effect of ischaemia, endothelin-1 and endothelin-1 antagonist BQ 610. *J Mol Cell Cardiol* 29: 3115–3122, 1997.

10. **Ingwall JS, Kramer MF, Fifer MA, Lorell BH, Shemin R, Grossman W, and Allen PD.** The creatine kinase system in normal and diseased human myocardium. *N Engl J Med* 313: 1050–1054, 1985.
11. **Kaasik A, Veksler V, Boehm E, Novotova M, Minajeva A, and Ventura-Clapier R.** Energetic crosstalk between organelles: architectural integration of energy production and utilization. *Circ Res* 89: 153–159, 2001.
12. **Kober F, Iltis I, Cozzone PJ, and Bernard M.** Myocardial blood flow mapping in mice using high-resolution spin labeling magnetic resonance imaging: influence of ketamine/xylazine and isoflurane anesthesia. *Magn Reson Med* 53: 601–606, 2005.
13. **Maestri R, Milia AF, Salis MB, Graiani G, Lagrasta C, Monica M, Corradi D, Emanueli C, and Madeddu P.** Cardiac hypertrophy and microvascular deficit in kinin B2 receptor knockout mice. *Hypertension* 41: 1151–1155, 2003.
14. **Miyatake K, Yamagishi M, Tanaka N, Uematsu M, Yamazaki N, Mine Y, Sano A, and Hirama M.** New method for evaluating left ventricular wall motion by color-coded tissue Doppler imaging: in vitro and in vivo studies. *J Am Coll Cardiol* 25: 717–724, 1995.
15. **Nahrendorf M, Spindler M, Hu K, Bauer L, Ritter O, Nordbeck P, Quaschning T, Hiller KH, Wallis J, Ertl G, Bauer WR, and Neubauer S.** Creatine kinase knockout mice show left ventricular hypertrophy and dilatation, but unaltered remodeling post-myocardial infarction. *Cardiovasc Res* 65: 419–427, 2005.
16. **Neubauer S, Horn M, Naumann A, Tian R, Hu K, Laser M, Friedrich J, Gaudron P, Schnackerz K, Ingwall JS, and Ertl G.** Impairment of energy metabolism in intact residual myocardium of rat hearts with chronic myocardial infarction. *J Clin Invest* 95: 1092–1100, 1995.
17. **Ruff J, Wiesmann F, Hiller KH, Voll S, von Kienlin M, Bauer WR, Rommel E, Neubauer S, and Haase A.** Magnetic resonance microimaging for noninvasive quantification of myocardial function and mass in the mouse. *Magn Reson Med* 40: 43–48, 1998.
18. **Small EM and Krieg PA.** Molecular regulation of cardiac chamber-specific gene expression. *Trends Cardiovasc Med* 14: 13–18, 2004.
19. **Spindler M, Meyer K, Stromer H, Leupold A, Boehm E, Wagner H, and Neubauer S.** Creatine kinase-deficient hearts exhibit increased susceptibility to ischemia-reperfusion injury and impaired calcium homeostasis. *Am J Physiol Heart Circ Physiol* 287: H1039–H1045, 2004.
20. **Starling RC, Hammer DF, and Altschuld RA.** Human myocardial ATP content and in vivo contractile function. *Mol Cell Biochem* 180: 171–177, 1998.
21. **Streif JU, Herold V, Szimtenings M, Lanz TE, Nahrendorf M, Wiesmann F, Rommel E, and Haase A.** In vivo time-resolved quantitative motion mapping of the murine myocardium with phase contrast MRI. *Magn Reson Med* 49: 315–321, 2003.
22. **Streif JU, Nahrendorf M, Hiller KH, Waller C, Wiesmann F, Rommel E, Haase A, and Bauer WR.** In vivo assessment of absolute perfusion and intracapillary blood volume in the murine myocardium by spin labeling magnetic resonance imaging. *Magn Reson Med* 53: 584–592, 2005.
23. **Urheim S, Edvardsen T, Torp H, Angelsen B, and Smiseth OA.** Myocardial strain by Doppler echocardiography. Validation of a new method to quantify regional myocardial function. *Circulation* 102: 1158–1164, 2000.
24. **Waller C, Hiller KH, Kahler E, Hu K, Nahrendorf M, Voll S, Haase A, Ertl G, and Bauer WR.** Serial magnetic resonance imaging of microvascular remodeling in the infarcted rat heart. *Circulation* 103: 1564–1569, 2001.
25. **Waller C, Hiller KH, Voll S, Haase A, Ertl G, and Bauer WR.** Myocardial perfusion imaging using a non-contrast agent MR imaging technique. *Int J Card Imaging* 17: 123–132, 2001.
26. **Wang M, Yip GW, Wang AY, Zhang Y, Ho PY, Tse MK, Yu CM, and Sanderson JE.** Tissue Doppler imaging provides incremental prognostic value in patients with systemic hypertension and left ventricular hypertrophy. *J Hypertens* 23: 183–191, 2005.
27. **Weidemann F, Breunig F, Beer M, Sandstede J, Stork S, Voelker W, Ertl G, Knoll A, Wanner C, and Strotmann JM.** The variation of morphological and functional cardiac manifestation in Fabry disease: potential implications for the time course of the disease. *Eur Heart J* 26: 1221–1227, 2005.
28. **Yang Z, Bove CM, French BA, Epstein FH, Berr SS, DiMaria JM, Gibson JJ, Carey RM, and Kramer CM.** Angiotensin II type 2 receptor overexpression preserves left ventricular function after myocardial infarction. *Circulation* 106: 106–111, 2002.